

# Synthesis and magnetic-electronic characterization of mixed-valence $\text{LuFe}_2\text{O}_{4-\delta}$ : effect of stoichiometry $\delta$

M A Peck<sup>1,2</sup>, W N Sibanda<sup>1</sup>, G Diguet<sup>1</sup>, C Martin<sup>3</sup>, E Carleschi<sup>1</sup> and G R Hearne<sup>1</sup>

<sup>1</sup>Department of Physics, University of Johannesburg, PO Box 524, Auckland Park, 2006, South Africa

<sup>2</sup>Department of Chemistry, University of Johannesburg, PO Box 524, Auckland Park, 2006, South Africa

<sup>3</sup>Laboratoire CRISMAT, ENSICAEN, UMR 6508 CNRS, Caen, France

Email: adlipeck@gmail.com

**Abstract.** Samples of  $\text{LuFe}_2\text{O}_{4-\delta}$  of varying oxygen stoichiometry ( $\delta$ ), prepared by solid state synthesis, have been characterised by x-ray diffraction,  $^{57}\text{Fe}$  Mössbauer-effect spectroscopy, SQUID magnetometry and transmission electron spectroscopy as well as electron-diffraction analysis. Magnetisation measurements show that the onset of ferrimagnetic ordering is confined to 245-250 K for the synthesised samples. Detailed analysis of Mössbauer spectra measured at variable cryogenic temperature confirm the mixed valence state and reveal the effects of charge and spin frustration of the triangular network of Fe atoms. The electron diffraction analysis demonstrates the existence of charge ordered superstructure (satellites) as well as an inhomogeneous distribution of oxygen throughout the lattice, irrespective of the  $\delta$  values.

## 1. Introduction

Multifunctional materials able to combine both magnetism and ferroelectric polarization, termed multiferroics, have strong potential for novel electronic functional devices [1]. This magneto-electric coupling offers manipulation of the electric polarization via a magnetic field and vice versa [2]. Rare-earth ferrites ( $R\text{Fe}_2\text{O}_4$ ) have been shown to exhibit this phenomenon, with a great deal of emphasis towards lutetium ferrite ( $\text{LuFe}_2\text{O}_4$ ) since Ikeda *et al.* showed the existence of a mixed-valence superstructure,  $\text{Fe}^{2+}/\text{Fe}^{3+}$  charge-ordering (CO), within these compounds [3]. There were initial claims that the CO is intimately linked to ferroelectric properties; however this has now been refuted and the electric polarization is now considered to be an extrinsic effect [4].

A review by Angst [4] highlights that due to the frustrated  $\text{LuFe}_2\text{O}_4$  lattice system, the triangular network of Fe atoms contains a number of degenerate charge and spin ordered states allowing transitions in both the magnetic and electric ordered dimensions. It has also been reported that oxygen-stoichiometry,  $\text{LuFe}_2\text{O}_{4+\delta}$ , plays a critical role in varying the physical and structural properties of this material. Both excess ( $\delta > 0$ ) [5, 6] and deficient ( $\delta < 0$ ) [7] samples lead to a suppression of the magnetic ordering volume and temperature ( $T_N$ ) as well as a deformation of the structural lattice. The mechanism of this variation as a function of the absence or excess of oxygen is still not fully understood. In this paper we will report on the synthesis and magnetic-electronic characterization of three oxygen-varied  $\text{LuFe}_2\text{O}_{4+\delta}$  samples and compare our results to those reported for excess and stoichiometric samples.

$\text{LuFe}_2\text{O}_4$  crystallizes in a rhombohedral lattice, consisting of an alternation of  $\text{LuO}_6$  monolayers with triangular networked  $\text{FeO}_5$  bi-layers (figure 1(a)), where Fe-O co-ordinates in a trigonal bipyramidal structure as indicated in figure 1(c), characteristic of these rare-earth ferrites [4]. Using high resolution transmission electron microscopy (TEM) and electron diffraction (ED) for samples with  $\delta < 0$  Yang *et al.* observed that a structural modulation occurred as well as local distortions in the  $b$ - $c$  plane and deformation of the  $\text{FeO}_5$  polyhedron, presumably affecting magnetic transitions [7]. A similar disruption of the stoichiometric lattice was observed by Hervieu *et al.* for samples where  $\delta > 0$ , in which case the cationic system expands to accommodate excess oxygen (up to  $\delta = 0.5$ ), resulting in a loss of the rhombohedral layer-stacking [5]. Their results point towards a reversible oxygen-storage application of  $\text{LuFe}_2\text{O}_4$  as well as the possibility to fine-tune  $\delta > 0$ . Previous Fe Mössbauer spectroscopy results show that  $\text{Fe}^{3+}/\text{Fe}^{2+}$  CO occurs below an onset temperature of  $T_{\text{CO}} = 320$  K [8] and above 370 K electron-hopping,  $\text{Fe}^{2+} \leftrightarrow \text{Fe}^{3+}$ , destroys the mixed-valence superstructure (CO melting) [9]. Stoichiometric samples show a paramagnetic to ferrimagnetic transition at  $T_{\text{N}} \approx 250$  K [8, 9] whilst off-stoichiometric samples show a suppression of  $T_{\text{N}}$  to below 250 K [5-7]. An antiferromagnetic transition also occurs at 175 K for all samples, while only off-stoichiometric samples display spin-glass magnetic behaviour at lower temperatures,  $T_{\text{LT}} < 175$  K [6, 7].

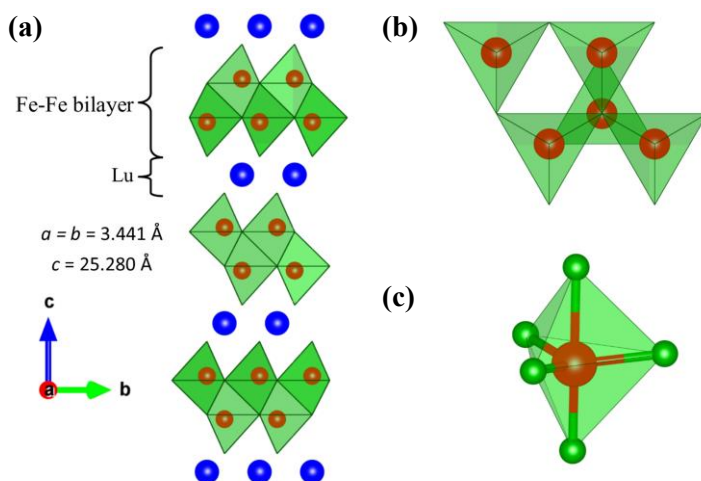


**Figure 1 (colour online):** (a) Rhombohedral lattice,  $R3\text{-}m$ , of  $\text{LuFe}_2\text{O}_4$  viewed in the  $b$ - $c$  plane (b) View down the  $c$ -axis of a single bilayer showing the triangular network of Fe atoms. (c) Five-fold coordination of Fe-O. Lu atoms are shown in blue, Fe in red and O atoms, at the vertices of the trigonal bipyramid, are shown in green.

## 2. Experimental

Two  $\text{LuFe}_2\text{O}_4$  polycrystalline powdered samples, enriched to 10 - 14%  $^{57}\text{Fe}$ , were prepared by solid-state reaction of starting mixtures according to the stoichiometric ratio  $0.50\text{Lu}_2\text{O}_3 : 0.83\text{Fe}_2\text{O}_3 : 0.34\text{Fe}$ . Mixtures were thoroughly ground in an agate mortar, pestled and compressed into 20 mg and 100 mg pellets. The pellets were vacuum-sealed in a quartz ampoule to  $3 \times 10^{-6}$  mbar before heating at 1100 °C for 12 hrs. A third sample with  $\delta \approx 0$  (designated MP), prepared on a gram-scale via a similar method, was received from Martin's group at the *Laboratoire Crismat, Caen, France* [5, 10]. This was also characterized and compared to our two synthesized samples.

Structural characterization was performed on synthesized samples by X-ray powder diffraction (XRPD) using a *Phillips X-Pert Pro* instrument with  $\text{Cu-K}\alpha$  radiation. Magnetic susceptibility measurements were carried out in a SQUID (QD: MPMS) in the temperature range 150 – 300 K.  $^{57}\text{Fe}$  Mössbauer effect spectroscopy (MES) measurements in transmission mode were conducted using a 10 mCi  $^{57}\text{Co}(\text{Rh})$  source and all samples were characterized with respect to a 25  $\mu\text{m}$   $\alpha$ -Fe-foil reference. Low temperature measurements were performed in a top-loading cryostat with the source and sample at the same temperature.

In addition electron diffraction measurements were performed on micron-dimensioned grains in a TEM, similar to those indicated in references [5, 10].

### 3. Results and discussion

#### 3.1. XRPD

Of the two synthesized samples, the diffraction pattern for the 20 mg sample showed a significant amount of impurities, (indicated by arrows in figure 2(b)) relative to the 100 mg sample. Sample MP's diffraction pattern (not shown here, see reference [5]) showed no discernible impurity phases either. Since sample MP was produced on a gram-scale, a possible inverse proportionality mass-purity effect takes place leading to unreacted material. This can also be observed in the Mössbauer spectrum of the 20 mg sample (figure 2(c)), which shows evidence of remnant  $\text{Fe}_3\text{O}_4$  and Fe impurity phases (as indicated by arrows) from the reaction sequence, not observed in the MP and 100 mg samples (see figure 3).

The crystal structure was resolved by Rietveld refinement and a best-fit, rhombohedral cell, with  $R3\text{-}m$  space group was obtained with parameters  $a = b = 3.441 \text{ \AA}$  and  $c = 25.280 \text{ \AA}$ . This is in good agreement with previous reports [10] and the pattern in figure 2(a) closely matches that of phase-pure samples of references [5] and [9]. The MP sample has already been well characterized in previous reports [5].

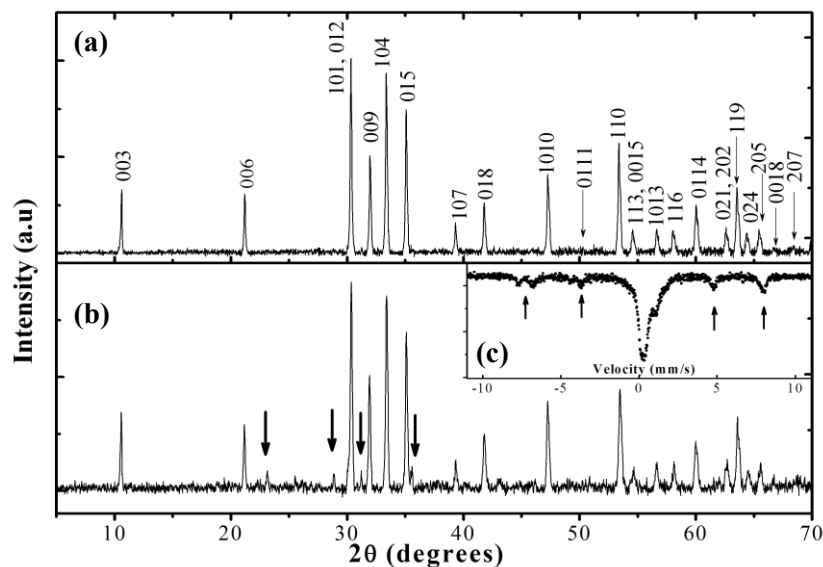


**Figure 2 (colour online):** XRPD data for (a) 100 mg and (b) 20 mg enriched  $\text{LuFe}_2\text{O}_4$  pellets. Inset (c) shows the MES spectrum of the 20 mg sample. Arrows indicate impurity phases.

#### 3.2. MES

Mössbauer spectra are shown for the MP and  $^{57}\text{Fe}$ -enriched 100 mg samples at room temperature in figure 3 and at 15 K in figure 4. At room temperature the spectra are commonly fitted as a combination of two doublets, corresponding to  $\text{Fe}^{2+}$  and  $\text{Fe}^{3+}$ , typical of the mixed-valence state [9]. However, for a best fit it was necessary to include a  $\text{Fe}^{3+}/\text{Fe}^{2+}$  electron-hopping (EH) component whilst allowing the isomer shifts and quadrupole splitting to correlate to those of the individual mixed-valence components. The fitting yields an electron exchange rate of  $\sim 2 \text{ MHz}$ . This likely occurs at CO domain boundaries or may be a result of CO frustration in the triangular network of figure 1(b). The abundance of the EH component in both samples is appreciable ( $\sim 20\%$ ) with the 100 mg sample (figure 3(b)) having a slightly smaller EH frequency in comparison with the MP sample. This is possibly due to the different oxygen stoichiometries in the two samples.

At 15 K (figure 4), where  $T \ll T_N$ , complex magnetic hyperfine structure is observed. The spectra were both fitted using six sextets allocating three potential sites for  $\text{Fe}^{3+}$  and two for  $\text{Fe}^{2+}$  [9], as well as a smeared  $\text{Fe}^{2+}$  component. This multiplicity of Fe sites is compatible with the known ferrimagnetic structure of the compound and the  $\text{Fe}^{2+}$  and  $\text{Fe}^{3+}$  superstructure (CO) that occurs in each sheet of a bilayer depicted in figure 1(a), as delineated in reference [4]. The model for each spectral component is calculated by solving the static Hamiltonian for mixed magnetic and quadrupole interactions using MOSSWINN [11]. The smeared component (broad linewidth, see last line of table 1) is supposed to

originate from disordered spins (fluctuating or a distribution of  $B_{hf}$  values), anticipated to occur in such a frustrated network, see figure 1(b). Longer-range magnetic exchange interactions within the bilayers give rise to the spin aligned (ordered) components. The parameters derived from the fitting of the MES spectra at 15 K are shown in table 1 and confirm that distinct charge states, mixed-valence  $Fe^{3+}$  and  $Fe^{2+}$ , occur; as compared to parameter values typical of ferrous and ferric iron [12]. It is interesting to note that the disordered spins comprise mainly  $Fe^{2+}$  moments.

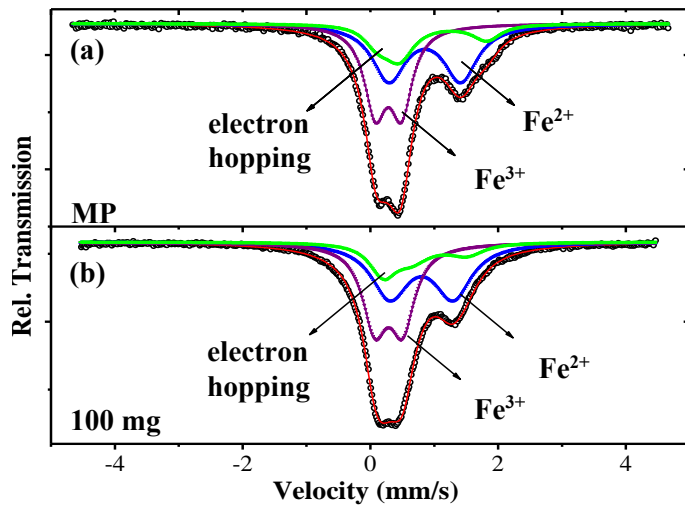


**Figure 3 (colour online):** Mössbauer spectra at RT for: (a) MP sample and (b) enriched 100 mg pellet.

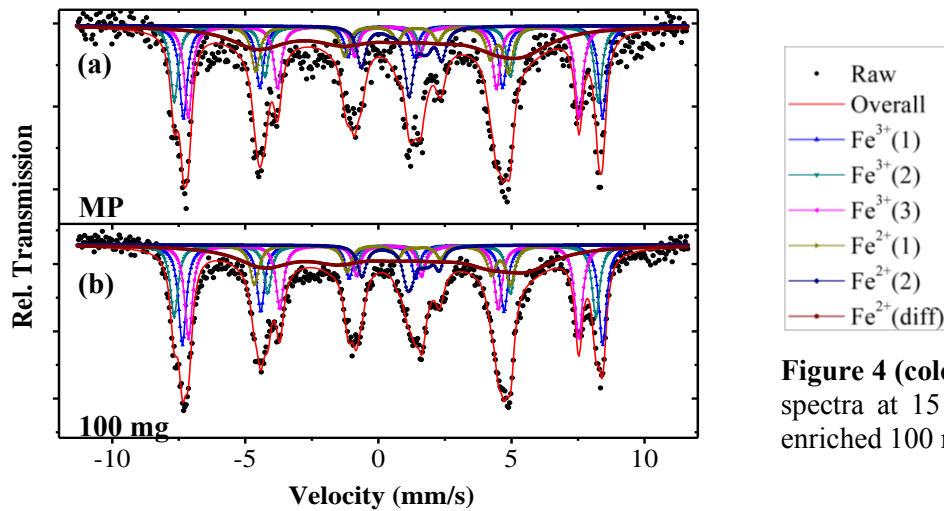


**Figure 4 (colour online):** Mössbauer spectra at 15 K for (a) MP and (b) enriched 100 mg pellet.

**Table 1:** MES parameters for the spectrum of the MP sample at 15 K. The isomer shift is  $\delta$  and Beta is the angle between the electric field gradient  $V_{zz}$  and the internal magnetic field at the Fe site,  $B_{hf}$ . A very similar tabulation has been obtained for the enriched 100 mg sample.

Site	$\Gamma$ line width <sup>a</sup> (mm/s)	$\delta / Fe$ (mm/s)	$B_{hf}$ (T)	$V_{zz} \times 10^{21}$ (V/m <sup>2</sup> )	$ 1/2 \cdot eQV_{zz} $ (mm/s)	Beta (deg)	Abundance (%)
$Fe^{3+}$ (1)	0.35	0.46	49	2.65	0.44	0	18
$Fe^{3+}$ (2)	0.35	0.45	50	-0.33	0.05	0	14
$Fe^{3+}$ (3)	0.35	0.39	45	-7.70	1.28	51	18
$Fe^{2+}$ (1)	0.41	0.93	29	-8.20	1.37	5	10
$Fe^{2+}$ (2)	0.41	1.13	6	-8.90	1.48	26	10
$Fe^{2+}$ (diff)	2.5	1.13	31	-6.50	1.08	0	30

<sup>a</sup>Fixed parameters

### 3.3. Magnetic susceptibility

Zero-field cooled magnetic susceptibility measurements on warming are given in figure 5 for the three samples.  $T_N$  has been determined from the point of inflection on the high temperature side of the peak. The 20 mg pellet shows a  $T_N$  of 247 K as well as a higher magnetic ordering volume, indicative of the impurity phases present. The 100 mg and MP sample show curves with a  $T_N$  of 249 and 255 K, respectively. The differences in  $T_N$  are due to differences in oxygen stoichiometry  $\delta$  of the two samples [5-7]. The MP sample has  $\delta \sim 0$  and the decrease in  $T_N$  in the enriched sample is attributed to a slight oxygen deficiency [7], which is in the process of being quantified by means of TGA measurements. The as received MP sample shows an additional transition at  $\sim 210$  K believed to be a stabilization of one of the degenerate magnetic configurations [13]. This evidently does not occur in the off-stoichiometric sample.

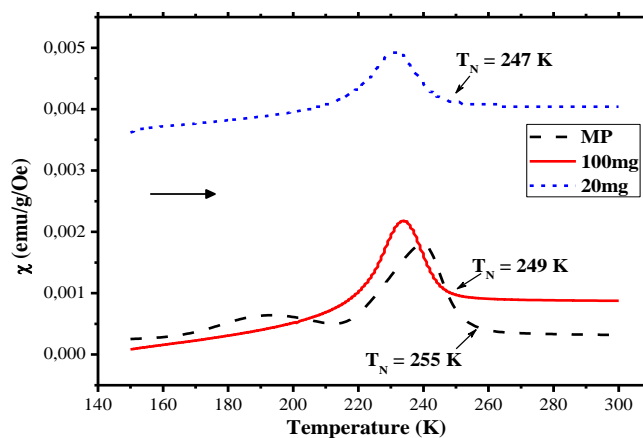


**Figure 5 (colour online):** Magnetic susceptibility for the  $^{57}\text{Fe}$ -enriched 20 and 100 mg samples, as well as for the MP sample.

### 3.4. TEM and ED

In the numerous papers devoted to this ferrite, ED patterns along the [100] axis are characterized by additional reflections leading to commensurate or incommensurate modulation vectors; all the authors agree that they are the signatures of CO [5, 10]. ED from high resolution TEM studies were taken for the 100 mg  $^{57}\text{Fe}$  enriched sample and compared to the as received MP sample.

Along the [100] axis in the MP sample (figure 6(a)), three modulation vectors are observed:  $\mathbf{q}_2$  ( $1/3 - \varepsilon$   $1/3 - \varepsilon$   $1/3$ ),  $\mathbf{q}_2'$  by twinning and  $\mathbf{q}_3$  ( $1/3$   $1/3$   $1/2$ ). The point-like satellites are rather intense, however weaker or rather diffuse satellites are also observed due to the  $C2/m$  sub-cell of  $R3-m$  [5]. Similarly, in the 100 mg enriched sample (figure 6(b)) weak zigzagging diffuse lines are observed (highlighted by the red arrows), which are associated with the  $\mathbf{q}_2$ ,  $\mathbf{q}_2'$  and  $\mathbf{q}_3$  vectors previously reported. This is similar to the MP samples (likely with short range charge ordered domains); except more intense satellites are present in the MP sample.

Along [010], the ED patterns of the 100 mg (figure 6(c)) and MP samples exhibit either no extra reflections, consistent with the  $C2/m$  structure, or there are satellites associated with an incommensurate modulated structure. The latter ones have been shown to be correlated with the formation of “oxidized” domains present in the matrix [5]; thus considered to be a true signature of a local excess of oxygen. The 100 mg sample thus shows an inhomogeneous distribution of oxygen throughout the lattice, as is the case in the MP sample (not shown here).

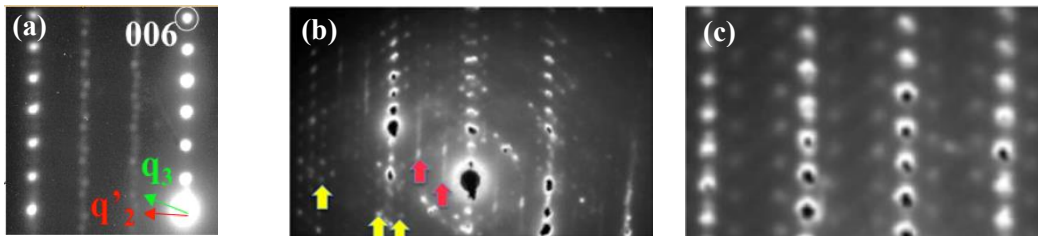


**Figure 6 (colour online):** ED patterns of (a) MP sample and (b) 100 mg enriched sample, along the [100] axis. Satellites from CO superstructure are emphasized by the red arrows; these are more intense in (a) and much weaker but nevertheless discerned in (b). Yellow arrows indicate unknown point-like satellites. (c) ED pattern for the 100 mg enriched sample along the [010] axis, showing satellites correlated to locally oxidized domains.

#### 4. Conclusions

We are able to prepare small quantities of  $^{57}\text{Fe}$  isotopically enriched mixed-valence  $\text{LuFe}_2\text{O}_{4-\delta}$  samples in which CO prevails. Such isotopic enrichment is imperative for future envisaged MES studies under high pressure. These are phase pure materials when a minimal amount of  $\sim 100$  mg is synthesized; there are slight deviations of oxygen stoichiometry from ideal  $\delta \sim 0$  values. Oxygen stoichiometry may readily be altered by a mild heat treatment (150 - 200 °C) in air [5]. In both stoichiometric and off-stoichiometric samples oxygen is inhomogeneously distributed in the lattice; there being oxidized domains with a local excess of oxygen. The degree of off-stoichiometry does not drastically alter the magnetic-electronic properties as exemplified by the magnetization and Mössbauer characterizations. These results have been compared to those for a well-characterized reference sample ( $\delta \sim 0$ ).

We have conducted a more comprehensive data analysis of the Mössbauer spectra than in the previous literature. The effects of geometrical charge and spin frustration, anticipated for such a triangular networked lattice structure, have been discerned in this detailed analysis by way of a residual electron-hopping component at  $T < T_{\text{CO}}$  and disordered spins at  $T \ll T_{\text{N}}$ , respectively.

#### References

- [1] Bibes M and Barthélémy A 2008 *Nat. Mater.* **7** 425-6
- [2] Béa H, Gajek M, Bibes M and Barthélémy A 2008 *J. Phys.: Condens. Matter* **20** 434221 (1-11)
- [3] Ikeda N, Ohsumi H, Ohwada K, Ishii K, Inami T, Kakurai K, Murakami Y, Yoshii K, Mori S and Horibe Y 2005 *Nature* **436** 1136 (1 - 3)
- [4] Angst M 2013 *Phys. Status Solidi RRL* **7** 383-400
- [5] Hervieu M, Guesdon A, Bourgeois J, Elkaïm E, Poienar M, Damay F, Rouquette J, Maignan A and Martin C 2014 *Nat. Mater.* **13** 74-80
- [6] Wang F, Kim J, Gu G D, Lee Y, Bae S and Kim Y-J 2013 *J. Appl. Phys.* **113** 063909 (1 - 7)
- [7] Yang H X, Tian H F, Wang Z, Qin Y B, Ma C, Li J Q, Cheng Z Y, Yu R and Zhu J 2012 *J. Phys.: Condens. Matter* **24** 435901 (1 - 7)
- [8] Xu X, Angst M, Brinzari T, Hermann R P, Musfeldt J, Christianson A D, Mandrus D, Sales B, McGill S and Kim J-W 2008 *Phys. Rev. Lett.* **101** 227602 (1 - 4)
- [9] Bang B K, Kouh T and Kim C S 2008 *J. Appl. Phys.* **103** 07E307 (1 - 3)
- [10] Rouquette J, Haines J, Al-Zein A, Papet P, Damay F, Bourgeois J, Hammouda T, Doré F, Maignan A and Hervieu M 2010 *Phys. Rev. Lett.* **105** 237203 (1 - 4)
- [11] Klencsár Z 2013 Mössbauer fitting program: *MOSSWINN* 4.0 <http://www.mosswinn.com/>
- [12] Gütlich P, Bill E and Trautwein A X 2011 *Mössbauer Spectroscopy and Transition Metal Chemistry: Fundamentals and Applications* (Berlin: Springer)
- [13] Christianson A D, Lumsden M D, Angst M, Yamani Z, Tian W, Jin R, Payzant E A, Nagler S E, Sales B C and Mandrus D 2008 *Phys. Rev. Lett.* **100** 107601 (1 - 4)